JOURNAL OF MAGNETIC RESONANCE, Series A 110, 170–174 (1994)

Relaxation-Time Measurement and Imaging in the Earth's Magnetic Field

G. PLANINŠIČ, J. STEPIŠINK, AND M. KOS

University of Ljubljana, Oddelek za fiziko FNT, Jadranska 19, 61000 Ljubljana, Slovenia

Received February 21, 1994

Investigation of nuclear magnetic relaxation-time imaging and measurement in the earth's magnetic field using field-cycling spin preparation has been performed. A new pulse technique named magnetization subtraction, which is equivalent to inversion recovery in a strong magnetic field, is introduced. Two new techniques for single-scan measurement of spin–lattice relaxation times in the earth's magnetic field are described. The results of image weighting with relaxation times in the earth's magnetic field are presented for the first time. © 1994 Academic Press, Inc.

INTRODUCTION

Most MR imaging experiments are conducted in relatively strong magnetic fields ranging from 0.1 to 3 T. The obvious reason for this is that the S/N ratio is proportional to the Larmor frequency. On the other hand it is well known that relaxation rates $1/T_1$ of different biological tissues exhibit strong dispersion at very low Larmor frequencies. It has been shown with different rat tissues (*1*) that $1/T_1$ dependence on B_0 has an inflection at values of B_0 that are typically below 0.01 T, therefore in a magnetic field range not covered by conventional MR tomography. Imaging of relaxation-time distribution in very weak magnetic fields may give additional information that cannot be obtained by strong-field MRI.

Our experiments were conducted in the earth's magnetic field. The low magnetic field density (0.5 G) and excellent homogeneity (better then 10^{-6} at the place of our apparatus, about 20 m away from the first building) provide a special condition for MRI experiments. The idea of MRI in the earth's magnetic field was based on some early NMR experiments performed in the earth's field (*2, 3*). The first reports on earth's field MRI appeared in 1985 independently by J. Stepišnik *et al.* (*4*) and H. Mehier *et al.* (*5*), but the first images of water samples and plants were shown by Stepišnik *et al.* a few years later (*6, 7*). The same group also showed the results of diffusion and flow measurements (*8*) and recently the results of relaxation-time imaging (*9–11*).

METHODS

The basic NMR experiment in the earth's magnetic field is in principle a field-cycling experiment. The sample is magnetized in a relatively strong magnetic field B_M (500 G in our case) perpendicular to the earth's field direction. The magnetization field is then adiabatically switched off, leaving the net magnetization pointing in the direction of the residual earth's magnetic field B_0^E (0.5 G in our case). If now a 90° pulse of oscillating magnetic field B_1 is applied, the FID signal can be detected with amplitude

$$U_{FID} \propto \left[1 - \exp\left(-\frac{t_m}{T_1^M}\right)\right]\exp\left(-\frac{t_d}{T_1^E}\right)\exp\left(-\frac{t}{T_2^E}\right), \quad [1]$$

where superscripts M and E indicate the relaxation in the magnetization field and in the earth's field, respectively. The meaning of the time intervals t_m and t_d is indicated in Fig. 1 and the time origin ($t = 0$) is set at the 90° pulse.

Note that the signal amplitude depends on three relaxation times and that the free precession decays with pure T_2^E, because of the excellent earth-field homogeneity. Equation [1]

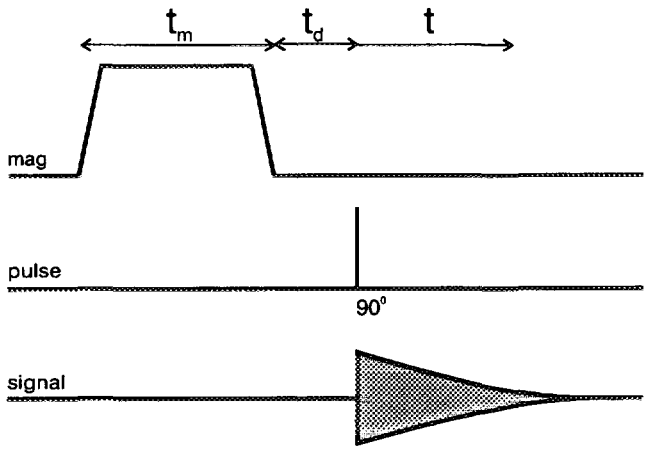

FIG. 1. Spin preparation for the earth's field NMR experiment.

1064-1858/94 $6.00
Copyright © 1994 by Academic Press, Inc.
All rights of reproduction in any form reserved.

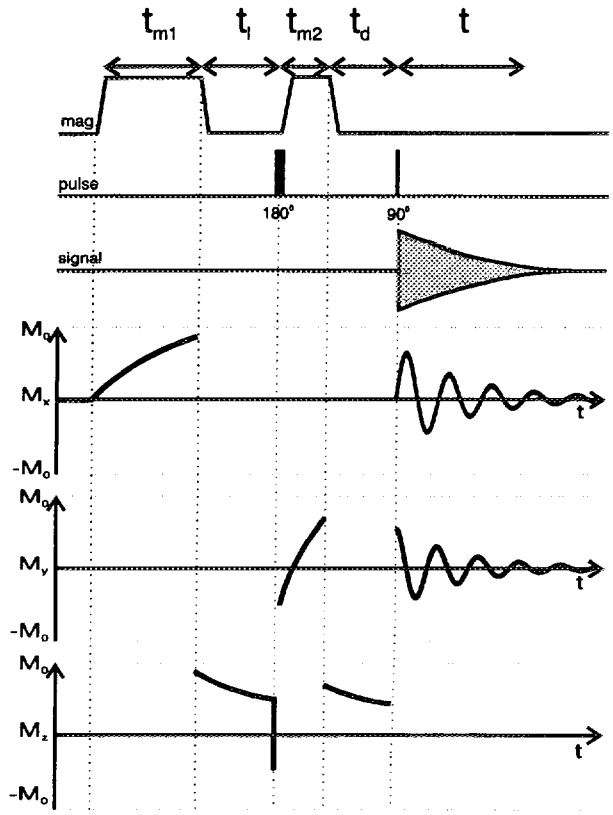

FIG. 2. The magnetization subtraction pulse sequence.

gives a means of measuring the three relaxation times. The relaxation time T_1^M can be determined by varying t_m (while keeping t_d and t constant) and fitting the data to an exponential function. Similarly T_1^E can be determined by varying t_d (t_m, t constant). T_2^E can be obtained simply from a single FID envelope. A combination of the spin preparation sequence described above and conventional spin manipulation with magnetic field gradients gives a basic sequence for MR imaging in the earth's magnetic field, which has been described elsewhere (*12*). A variation of time intervals t_m, t_d and the position of the spin echo will produce T_1^M-, T_1^E-, and T_2^E-weighted images, but in order to use the advantages of low fields, more specialized weighting techniques were developed.

A very useful technique for T_1 contrast manipulation in strong-field MRI is the inversion-recovery technique. An analogous technique also exists for earth-field MRI. Let B_M and B_1 be parallel to x and B_0^E be parallel to the z axis. The pulse sequence (without imaging gradients) and corresponding evolution of sample magnetization are shown in Fig. 2. The basic idea is to employ two magnetization periods with the magnetization field in the same direction, and to change the direction of the sample magnetization to be opposite to this field during the second magnetization. The

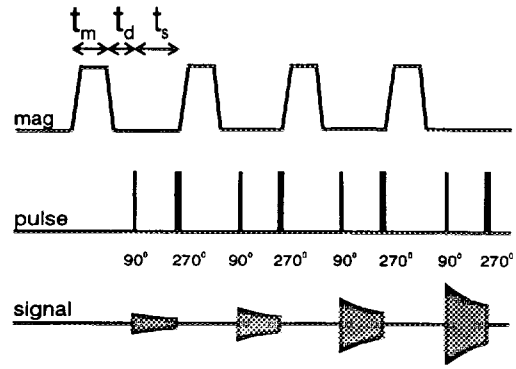

FIG. 3. Pulse sequence for single-scan T_1^M measurement.

effect of the second magnetization is to decrease and then again increase the sample magnetization, depending on its duration—very much like the effect of the 180°–90° time interval in the inversion-recovery technique.

We have named this technique *magnetization subtraction*. The important parts of the magnetization subtraction technique are adiabatic switches of the magnetization field, while the net magnetization precesses around the direction of the resultant field. This is the effect that causes sample magnetization to change in the opposite direction to B_M during the second magnetization switch-on. The signal amplitude immediately after the 90° pulse is, for the completely magnetized sample when $t_{m1} > 5T_1^M$

$$U_{FID} \propto \left\{1 - \exp\left(-\frac{t_{m2}}{T_1^M}\right)\left[1 + \exp\left(-\frac{t_1}{T_1^E}\right)\right]\right\} \times \exp\left(-\frac{t_d}{T_1^E}\right). \quad [2]$$

The technique can be applied to determine T_1^M or T_1^E by fitting the data to exponential functions: signal amplitudes obtained for different t_{m2} values are described by a function of the form

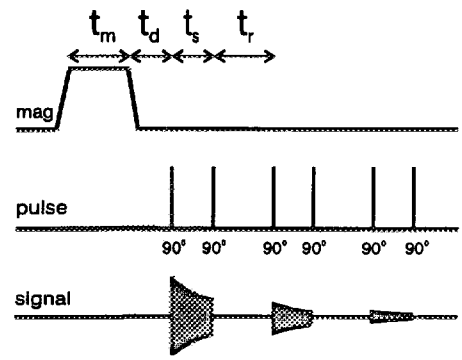

FIG. 4. Pulse sequence for single-scan T_1^E measurement.

TABLE 1
The Relaxation Times of Gelatins Used in a Phantom

	0.5 G (ms)	500 G (ms)	2.34 T (Bruker system) (ms)
Gel 1 (70 g/liter)	$T_1^E = 800$ $T_2^E = 850$	$T_1^M = 1030$	$T_1 = 2300$ $T_2 = 450$
Gel 2 (150 g/liter)	$T_1^E = 390$ $T_2^E = 360$	$T_1^M = 800$	$T_1 = 2330$ $T_2 = 480$

Note. The relaxation times in 0.5 and 500 G fields were measured with methods described in this article. The relaxation times in a 2.34 T field were obtained with standard methods. The errors for data in the table are not more than 10%.

$$1 - A \exp(-t_{m2}/T_1^M),$$

and scanning through different t_I values gives signal amplitudes that are described by a function of the form

$$(1 - B) - B \exp(-t_I/T_1^E),$$

where $A = 1 + \exp(-t_I/T_1^E)$ and $B = \exp(-t_{m2}/T_1^M)$ are constants through each experiment. Note that both functions cross the zero signal point.

Due to excellent B_0^E homogeneity, the FID signal decays with pure T_2^E, giving enough time to perform multiple spin manipulations in a single scan, as shown in Fig. 3. The basic idea of this pulse sequence is to observe a gradual increase in the longitudinal magnetization in the B_M field during a single experiment. The observations start with 90° pulses and terminate with 270° pulses. The role of the 270° pulse is to rotate the net magnetization in the B_0^E direction, from

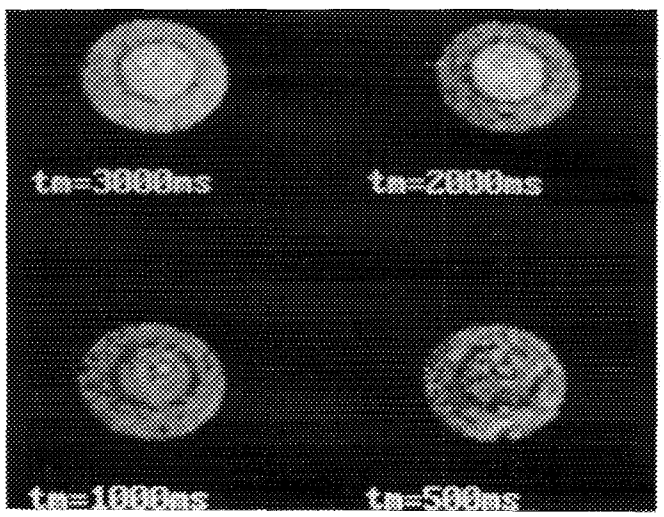

FIG. 5. T_1^M-weighted images.

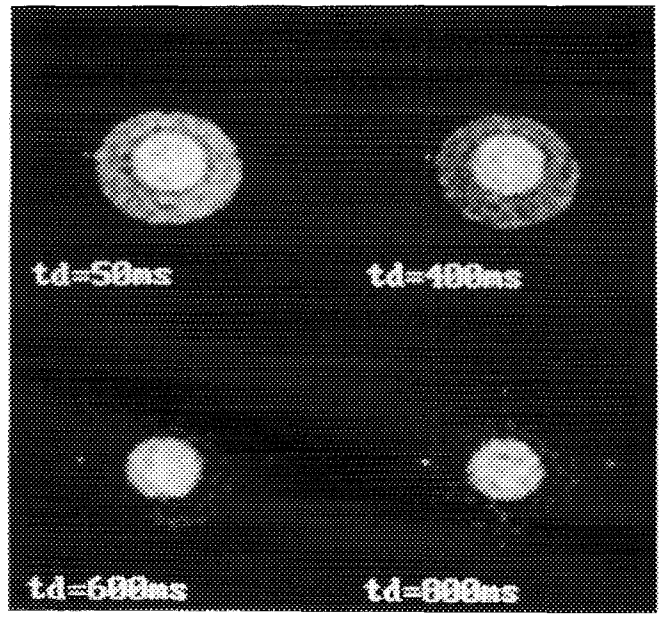

FIG. 6. T_1^E-weighted images.

where the adiabatically switched magnetization field turns it in the B_M direction, adds some magnetization, and turns it back in the B_0^E direction. The nth amplitude of the observed signal immediately after a 90° pulse is

$$U_n \propto (1 - E_m)E_a \frac{1 - (E_m E_a E_s)^n}{1 - E_m E_a E_s}, \qquad [3]$$

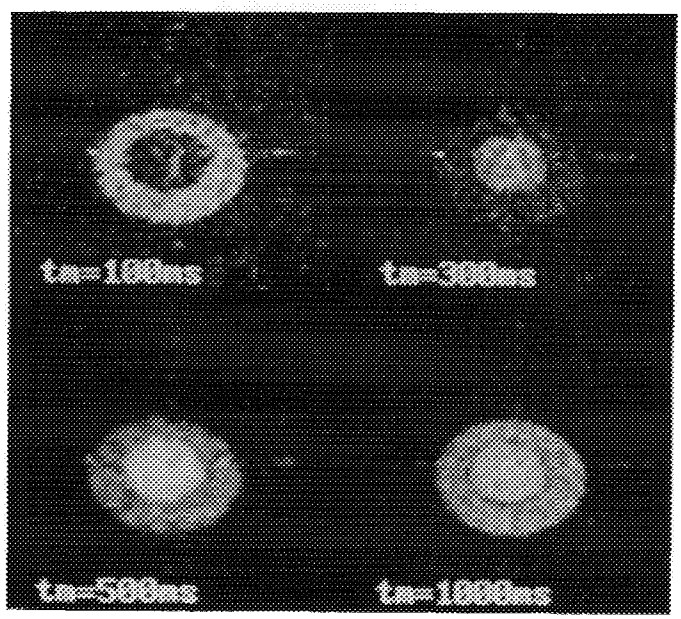

FIG. 7. Magnetization subtraction: images weighted with second magnetization.

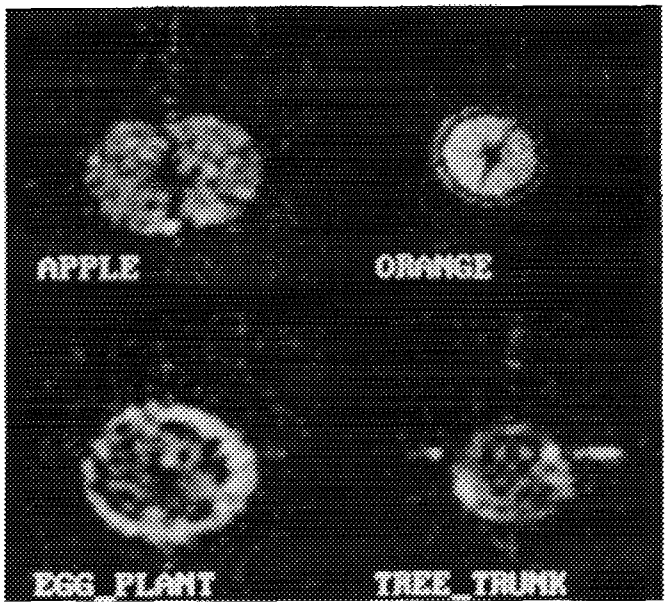

FIG. 8. Images of some plants obtained with the earth's field MRI.

where

$$E_m = \exp\left(-\frac{t_m}{T_1^M}\right), \quad E_a = \exp\left(-\frac{t_d}{T_1^E}\right), \quad E_s = \exp\left(-\frac{t_s}{T_2^E}\right).$$

If $nt_d \ll T_1^E$ (a condition fulfilled for first few signals), Eq. [3] takes the simplified form

$$U_n \propto (1 - E_m)\frac{1 - (E_m E_s)^n}{1 - E_m E_s}. \quad [4]$$

Since T_2^E can be determined from signal envelopes, both T_2^E and T_1^M can be measured in a single scan. The equivalent pulse sequence for single-scan T_1^E measurement is shown in Fig. 4.

The decay of longitudinal magnetization of the sample in the earth's magnetic field is sampled by odd 90° pulses and turned parallel to the B_0^E direction by even 90° pulses. With neglect of sample magnetization in the earth's magnetic field, the nth amplitude of the observed signal after odd 90° pulses is proportional to

$$U_n \propto (1 - E_m)E_a(-E_s E_r)^{n-1}, \quad [5]$$

where $E_r = \exp(-t_r/T_1^E)$. For a completely magnetized sample and for $t_d \ll T_1^E$, Eq. [5] takes the simplified form

$$U_n \propto (-E_s E_r)^{n-1}, \quad [6]$$

which indicates that T_1^E and T_2^E can be measured in a single scan under the given conditions.

RESULTS

Image-weighting techniques as described above were tested on a gelatin phantom. The phantom consisted of two concentric cylindrical containers (outer dimension, 9 cm) filled with gelatin mixtures of different concentrations. T_1 values for both gelatins (Table 1) were determined from the exponential fit of the results obtained from FID measurements (Fig. 1). The results of T_1^M and T_1^E weighting are shown in Figs. 5 and 6, respectively. The former is achieved by changing t_m and the latter by changing t_d. Note the significant contrast enhancement in T_1^E-weighted images. The results of magnetization subtraction are shown in Fig. 7. The value of t_m shows the duration of the second magnetization. Signal void in the inner container (t_m = 100 ms) and inverted contrast are clearly visible. In all cases the signals were recorded on a 64 × 64 matrix with a 10-bit ADC. The images presented were obtained, using typically eight averages, in about 30 minutes. The resolution of our system can be estimated from images of some plants in Fig. 8.

CONCLUSIONS

Direct relaxation-time measurements and weighted MR images of gelatin phantoms in the earth's magnetic field confirm increased differences between T_1 values of different substances in a very weak magnetic field. These differences appear particularly pronounced in the kilohertz Larmor frequency range, roughly matching typical rotational frequencies of large protein molecules. In addition, three new pulse techniques were developed for field-cycling relaxation-time measurements and imaging in the earth's magnetic field: magnetization subtraction, which is equivalent to the inversion-recovery technique, and two single-scan techniques for fast spin–lattice relaxation time measurements. All techniques are, however, applicable only to samples with relatively long T_2^E times (not shorter than 200 ms for the present system).

The results show that earth's field MR may play an important role in the study of large-molecule dynamics, in applications where image contrast rather than resolution is of primary interest, and also in imaging of very large samples.

ACKNOWLEDGMENTS

The authors thank Mr. Vital Eržen for his technical contributions. G.P. thanks the Slovenian Ministry for Science and Technology for funding his Ph.D. studies, of which this work is part.

REFERENCES

1. S. H. Koenig, D. Adams, D. Emerson, and C. G. Harrison, Research Report RC 10116, IBM Research Division, 1983.

2. M. Packard and R. Varian, *Phys. Rev.* **93,** 941 (1954).
3. G. J. Bene, B. Borcard, E. Hiltbrand, and P. Magnin, *Philos. Trans. R. Soc. London B* **289,** 501 (1980).
4. J. Stepišnik and D. Mihailovič, 7th Specialized Coloque AMPERE, Bucharest, p. 194, 1985.
5. H. Mehier, M. Maurice, J. P. Bonche, G. Jacquemod, C. Desuzinges, B. Favre, and J. O. Peyrin, *J. Biophys. Biomec.* **9,** 198 (1985).
6. J. Stepišnik, V. Eržen, M. Kos, and G. Planinšič, Abstracts of the Society of Magnetic Resonance in Medicine, 7th Annual Meeting, San Francisco, p. 1060, 1988.
7. J. Stepišnik, V. Eržen, M. Kos, G. Planinšič, and P. Pogačnik, *Phys. Medica* **6,** 235 (1990).
8. J. Stepišnik, M. Kos, and G. Planinšič, 11th EENC Conference, Lisbona, p. 211, 1992.
9. G. Planinšič, J. Stepišnik, M. Kos, and V. Eržen, 11th ESMRMB Conference, Rome, p. 90, 1993.
10. G. Planinšič, J. Stepišnik, M. Kos, and V. Eržen, AMPERE Summer Institute, Portorož, p. 213, 1993.
11. G. Planinšič, Ph.D. Thesis, Ljubljana, 1993.
12. J. Stepišnik, V. Eržen, and M. Kos, *Magn. Reson. Med.* **15,** 386 (1990).